ENVIRONMENTAL RESEARCH
LETTERS

LETTER • **OPEN ACCESS**

Hotspots of extreme runoff across Arctic land ice

IOP Publishing Environ. Res. Lett. 20 (2025) 104007 https://doi.org/10.1088/1748-9326/adfc80

ENVIRONMENTAL RESEARCH
LETTERS

OPEN ACCESS

RECEIVED
11 May 2025

REVISED
22 July 2025

ACCEPTED FOR PUBLICATION
18 August 2025

PUBLISHED
2 September 2025

LETTER

Hotspots of extreme runoff across Arctic land ice

Josep Bonsoms[1,*], Xavier Fettweis[2], Marc Oliva[1], Sergi González-Herrero[3] and Ignacio López-Moreno[4]

[1] Department of Geography, Universitat de Barcelona, Barcelona, Spain
[2] Department of Geography, SPHERES research unit, University of Liège, Liège, Belgium
[3] WSL Institute for Snow and Avalanche Research SLF, Davos, Switzerland
[4] Instituto Pirenaico de Ecología, Consejo Superior de Investigaciones Científicas (IPE–CSIC), Zaragoza, Spain
[*] Author to whom any correspondence should be addressed.

E-mail: josepbonsoms5@ub.edu

Keywords: Arctic, climate change, extreme events, runoff, climate extremes, Arctic amplification

Supplementary material for this article is available online

Abstract

The Arctic is warming at nearly three times the global average, driving profound shifts in its hydrological cycle. Yet, the impacts of this rapid warming on extreme runoff events—key to ice mass balance, ecosystem dynamics, and global climate feedbacks—remain poorly quantified. Here, we analyze the spatiotemporal evolution of summer extreme runoff across the permanent land ice Arctic area from 1980 to 2020 based on high-resolution regional climate model simulations (MARv3.11). Extreme runoff is defined as summer runoff exceeding the 90th, 95th, or 99th percentile of modeled runoff distributions, consistent with established climate extreme thresholds. We then identify regional hotspots and quantify changes in the fraction of extreme runoff relative to total summer runoff, as well as shifts in its magnitude and drivers. Greenland contributes to most of the land ice Arctic extreme runoff area, accounting for 63% of the total, followed by Baffin (14%) and Ellesmere (8%). Our results reveal a marked intensification of extreme runoff, most notably in the Western Arctic. The fraction of extreme runoff has significantly increased, particularly in Greenland (+46%), Ellesmere (+38%), and Devon (+31%) (1980–2020 vs 2000–2020). In Ellesmere, the spatial extent of extreme runoff has expanded nearly 400%. Overall, the contribution of extreme runoff to total runoff increased by 20%–30% (1980–2020 vs 2000–2020) across the Arctic, with the largest increases in Ellesmere and Devon. A clear West-East gradient is evident, with statistically significant trends in the Western Arctic and more moderate changes in the East. For example, Iceland and Franz Josef Land show only modest increases in the fraction of extreme runoff (+11% and +2%, respectively). These patterns are consistent across multiple thresholds for extreme runoff (90th, 95th, and 99th percentiles) and remain robust after detrending. This intensification of extreme runoff is linked to increases in anticyclonic circulation in the Western Arctic. The results have far-reaching implications, including increased freshwater discharge into the Arctic Ocean and the potential disruption of the Atlantic Meridional Overturning Circulation.

1. Introduction

The Arctic is experiencing rapid cryosphere changes, characterized by a summer decrease in snow and ice cover and an associated increased in runoff (Callaghan *et al* 2011, Liston and Hiemstra 2011, Pulliainen *et al* 2020, IPCC 2022, Rantanen *et al* 2022). These changes contribute to a positive energy balance feedback, which further amplifies Arctic warming (IPCC 2022).

While the impacts of gradual Arctic warming are well-documented, extreme weather events—such as prolonged heatwaves, intense melt episodes, and extreme runoff events—are increasingly recognized for their profound impacts on Arctic ecosystems and human communities (Walsh *et al* 2020). The

magnitude and frequency of these events are often driven by complex interactions between atmospheric circulation patterns and surface-feedback processes (Bonsoms *et al* 2024). Persistent high-pressure systems have been linked to prolonged melt seasons and intensified surface melt across the region (Hanna *et al* 2014, Tedesco and Fettweis 2020, Sasgen *et al* 2024). Concurrently, reductions in sea ice have enhanced ocean-atmosphere heat exchange, further amplifying surface warming and accelerating melt processes (Chung *et al* 2021). This accelerated Arctic warming has resulted in record-breaking temperature extremes, such as the 2015–2016 Alaskan heatwave, which was attributed to a combination of low-albedo surface states and persistent high-pressure systems (Walsh *et al* 2017). A particularly striking example occurred from 28–30 July 2000, when an intense melt event at John Evans Glacier, Ellesmere Island accounted for approximately 30% of the glacier's total summer melt (Boon *et al* 2003). Similarly, in Canada's Queen Elizabeth Islands, 30%–48% of the total mass loss from four monitored glaciers since 1963 occurred after 2005, during years marked by extreme melt linked to anomalous summer atmospheric circulation and enhanced advection of warm air from the Northwest Atlantic (Sharp *et al* 2011). These events highlight the increasing role of extreme events in shaping the Arctic's cryosphere under rapid warming.

Projections indicate that Arctic temperatures and the frequency of extremes will continue to rise (Landrum and Holland 2020), with important implications for permafrost stability, infrastructure resilience, ecosystem health, and Arctic communities (Hansen *et al* 2014, Hjort *et al* 2018, Ford *et al* 2021, IPCC 2022, Miner *et al* 2022). Moreover, intensified glacier and snow melt in the Arctic is expected to trigger far-reaching impacts on global systems, including rising sea levels and cascading effects on mid-latitude weather patterns (Cohen *et al* 2014, Tang *et al* 2014, Francis and Skific 2015, Hanna *et al* 2017, Coumou *et al* 2018). Critically, it may also accelerate the approach to major climate tipping points, such as potential disruptions to the Atlantic Meridional Overturning Circulation (AMOC, Lenton *et al* 2008, Boers 2021).

Previous research on extreme Arctic melt events has largely concentrated on the Greenland Ice Sheet (GrIS) melting (Bonsoms *et al* 2024) or specific regions such as Canada's Arctic ice caps (Sharp *et al* 2011). While several pan-Arctic long-term (>20 years) studies have investigated temperature-related extremes—including marine heatwaves (Gou *et al* 2025), shifts in surface air temperature over land and ocean (Giesse *et al* 2024), warm and cold air outbreaks (Matthes *et al* 2016), and terrestrial heatwaves (Dobricic *et al* 2020)—temperature alone remains an indirect proxy for glacier and snow melt. In contrast, runoff represents a direct and physically meaningful metric, capturing the integrated effects of the surface energy balance and internal snow and firn processes, including refreezing. As such, it serves as a more accurate indicator of freshwater discharge and its consequences, including oceanographic fluxes, ecosystem impacts, and global climate (Fichot *et al* 2013, Nummelin *et al* 2016). Despite the increasing frequency and intensity of extreme climate events in the Arctic, no study has systematically quantified the spatial and temporal variability of extreme runoff across Arctic permanent land ice regions. This study addresses that gap by identifying Arctic summer extreme runoff hotspot regions and analyzing changes in their probability, magnitude, and spatial extent from 1980 to 2020. Using high-resolution data from a regional climate model (RCM), we present a comprehensive assessment of extreme runoff trends across the permanent land ice area of the Arctic.

The data sources and methodology used in this study are detailed in section 2. The results, with a focus on the probability, magnitude, and spatial distribution of extreme melt and runoff events across the Arctic are detailed in section 3. In section 4, we provide a discussion of the drivers behind regional variability and explore the broader implications of our findings for Arctic and global systems. Finally, section 5 offers key conclusions.

2. Data and methods

2.1. Data

Data from the RCM Modèle Atmosphérique Régional version 3.11 (MARv3.11) are used to analyze runoff across the Arctic region. The analysis focuses on the summer season, encompassing the months of June through August, for each year from 1980 to 2020. The analysis of data from 1979 onwards minimized biases associated with sparse observational data in earlier decades. MARv3.11 was run at a 6 km horizontal resolution over Arctic permanent land ice areas and was forced every 6 h using ERA5 reanalysis data. ERA5 assimilates *in situ* and satellite observations through a 4D-Var system with 137 vertical pressure levels (Hersbach *et al* 2020). The model configuration has been validated in Greenland (Delhasse *et al* 2020). The MARv3.11 permanent land ice Arctic dataset is provided at monthly temporal resolution by Maure *et al* (2023). MARv3.11 incorporates a hydrostatic atmospheric framework and includes a cloud microphysical scheme (Gallé and Schayes 1994). It is coupled with the soil ice snow vegetation atmosphere transfer module, which simulates runoff using the CROCUS model, a one-dimensional, multi-layer energy and mass balance model that includes for snow, firn and ice processes

(snow metamorphism, refreezing, liquid water percolation, and saturation, etc) (Brun *et al* 1992). MAR has been extensively validated against *in situ* measurements, passive microwave remote sensing data, and other RCMs for simulating climate and cryosphere processes in the Antarctic and GrIS (Fettweis *et al* 2020, Delhasse *et al* 2020, Maure *et al* 2023, and references therein). The MARv3.11 data used here was validated against satellite-derived records to simulate surface mass balance (SMB) for the period 2000–2020 (Hugonnet *et al* 2021) and against stake observations in GrIS (Machguth *et al* 2016). The model data were also validated against daily meteorological observations, demonstrating strong correlations (>0.8) for 2.m daily air temperature and wind speed biases within ± 1.5 m s^{-1}. In addition, MARv3.11 showed good agreement with SMB observational datasets across the Arctic, with correlations exceeding 0.93 (Maure *et al* 2023). These validations confirm the reliability of MARv3.11 in capturing the spatial and temporal variability of runoff across the Arctic.

To better understand extreme runoff trends and their link with atmospheric circulation, geopotential height at 500 hPa (Z500) from ERA5 reanalysis data (Hersbach *et al* 2020) is analyzed from 1980 to 2020, covering the region between 50°–85°N and 110°W–100°E.

2.2. Extreme runoff indicators and atmospheric circulation analysis

Extreme runoff events are analyzed during the summer months from 1980 to 2020, with a particular focus on changes between the 20 year periods: 1980–2000 and 2000–2020. Extreme runoff was defined using percentile-based thresholds, consistent with established methods for analyzing extreme temperature events in the Arctic (Matthes *et al* 2016, Dobricic *et al* 2020). Specifically, we adopted the 90th, 95th, and 99th percentiles to classify extreme runoff months, following the framework developed by the Expert Team on Climate Change Detection and Indices for identifying climate extremes. Main results are presented for the 90th percentile threshold, while sensitivity analysis using the 95th, and 99th percentiles are provided at supplementary materials and in figure 2. To capture the spatial and temporal variability of extreme runoff, we employed three key indicators, each reflecting distinct aspects of runoff intensity and distribution. (1) Fraction of extreme runoff: The number of months with extreme runoff during each summer season, expressed as a percentage of the total summer months (i.e. June, July and August). This metric represents the seasonal probability of extreme runoff events and is consistent with prior studies examining changes in the global probability of monthly temperature extremes (van der Wiel and Bintanja 2021). (2) Quantity: The total accumulated runoff during months classified as extreme. This indicator reflects the magnitude of freshwater discharge associated with extreme runoff events. (3) Spatial extent: The geographic area experiencing extreme runoff. This metric captures the spread or expansion of extreme runoff conditions across the permanent land ice Arctic domain.

Trends were assessed using the Mann–Kendall (MK) test, a non-parametric method that evaluates the presence of monotonic trends and is robust to outliers and distributional assumptions (Mann 1945, Kendall 1975). The MK test statistic, Kendall's tau (τ), measures the strength and direction of trends, and associated p-values indicate statistical significance. Regional trends were further classified as *high* or *low* based on whether τ values exceeded or fell below the mean (table S1). To estimate the magnitude of trends, we used the Sen's slope estimator (Sen 1968), which calculates the median of all pairwise slopes between data points, providing a robust measure of trend magnitude.

To address potential serial correlation, which can bias trend detection in hydrological time series, we validated MK and Sen's slope results using the trend-free prewhitening (TFPW) approach (Yue *et al* 2003). TFPW prewhitens the autocorrelation from the original series and then reintroduces the trend, reducing the risk of spurious significance.

Additionally, trend analyses were conducted on both detrended and non-detrended datasets to distinguish secular trends driven by long-term increases from those influenced by short-term variability or extreme runoff months. Detrending was performed by removing the linear summer runoff trend using least-squares regression. A detailed comparison of the trends obtained from the different methods and detrended analysis can be found in figures S1, S2, and table S1.

Spatial changes are analyzed and presented at the grid scale (figures 1 and 2), while aggregated trends are examined at the regional scale. At the regional scale, the total extreme runoff analysis is assessed by aggregating data for each region and subsequently subtracting extreme classifications and trends. The regionalization adopted in this study includes the Russian High Arctic Islands, Novaya Zemlya, Franz Josef Land, Svalbard, and Iceland, which collectively comprise the East Arctic. The West Arctic encompasses Greenland, Baffin Island, Devon Island, and Ellesmere Island. Note that Axel Heiberg Island is considered as part of the Ellesmere region. This delineation is consistent with previous studies on Arctic runoff and cryospheric processes (Maure *et al* 2023). Given that Greenland accounts for the majority of extreme runoff, an additional analysis was conducted to evaluate its elevation dependence. This involved assessing changes in the fraction of extreme runoff

across different elevation ranges. Furthermore, fraction of extreme runoff changes was aggregated by Greenland's sectors (Rignot and Mouginot 2012), with these sector boundaries extended linearly toward the ablation zone.

Summer Z500 (1980–2020) trend analysis was conducted using the same statistical method as for runoff, based on the Mann–Kendall trend test. Anomalies relative to the 1980–2000 period were calculated by subtracting the values of each year since 2000 from the 1980–2000 average. Weighted averages of ERA5 data were calculated using cosine latitude weighting to account for the Earth's spherical geometry, ensuring proper scaling of polar grid cells.

3. Results

3.1. Fraction of extreme runoff

The Arctic has experienced a marked intensification of extreme runoff events, with notable increases in the fraction, quantity and spatial extent of these events (figures 1–4). When comparing the periods 1980–2000 and 2000–2020, the fraction of extreme runoff has risen significantly across most regions. The most pronounced increases were observed in Greenland (+46%), Ellesmere Island (+38%), and Devon Island (+31%). In contrast, regions in the Eastern Arctic exhibited smaller anomalies, with Franz Josef Land (+2%) and Iceland (+11%) showing the lowest changes (figures 1 and 2(b)).

The statistical analysis of the temporal evolution in the fraction of extreme runoff, based on the Mann–Kendall trend test applied across multiple percentile thresholds (90th, 95th, and 99th) is shown in figure 2(c). Analyses were conducted using both raw (−R) and detrended (−D) data to differentiate between trends driven by long-term increases in runoff and those arising from intensified extreme runoff fraction. Western Arctic regions exhibit consistent and statistically significant trends in extreme runoff ($\tau \geqslant 4$, $p \leqslant 0.05$) at the 95th percentile in non-detrended data. Among these, Baffin and Ellesmere show the strongest trends ($\tau \geqslant 5, p < 0.05$), both for the 90th and 95th percentiles. When using detrended data, only Ellesmere continues to exhibit a statistically significant increase at the 95th percentile ($\tau = 6.1, p < 0.05$), suggesting a robust intensification of extreme runoff independent of long-term trends. Trend results were consistent across different analysis methods (figures S1 and S2; table S1).

In contrast to the Western Arctic, the Eastern Arctic sector displays generally weaker trends in extreme runoff. Only Novaya Zemlya and Svalbard exhibit statistically significant trends at the 95th percentile in the raw data ($\tau = 7.1$, $p < 0.05$). Svalbard also shows a statistically significant trend at the 99th percentile ($\tau = 6.6$, $p < 0.05$), while Franz Josef Land presents a non-statistically significant increase at the 99th percentile in raw data ($\tau = 6.2$, $p > 0.05$). Overall, trends in the Eastern Arctic are weaker than in the Western Arctic, with some regions even exhibiting declines. For instance, Novaya Zemlya shows a slight, non-statistically significant decrease at the 90th percentile in the detrended data ($\tau = -0.54$, $p = 0.82$). Iceland presents the weakest trends, with no statistically significant changes. Some indicators show weak or non-significant positive trends (e.g. 99th−D, $\tau = 3.3$, $p = 1.0$), while others suggest minimal or slightly negative trends (e.g. 95th−R, $\tau = -0.6$, $p = 1.0$).

3.2. Extreme quantity

The percentage contribution of total accumulated summer extreme runoff from each Arctic region is shown in figure 2(b). Greenland accounts for the majority of extreme runoff (63%), followed by Baffin (14%), Ellesmere (8%), and Devon (7%). All remaining regions contribute less than 3% individually. The intensification of extreme runoff is also evident in the total quantity of extreme runoff (figures 2(a) and (d)). The distribution of accumulated runoff during extreme events has shifted toward higher values in the 2000–2020 period, particularly across the Western Arctic, indicating a rise in the mean and frequency of high runoff years (figure 2(d)). The spatial expansion of areas affected by extreme runoff is further illustrated in figure 3. The largest modeled increases in extreme runoff quantity between the 1980–2000 and 2000–2020 periods are observed in Ellesmere (+33%), Devon (+32%), and Greenland (+27%). These changes reflect a shift in high-probability extreme runoff zones toward regions that were previously less affected, especially in the Western Arctic. Notably, the spatial extent of extreme runoff areas has increased dramatically in Ellesmere (+400%), followed by Baffin and Greenland (+320%) and Devon (+289%) over the same period (figure 2(a)). In contrast, the Eastern Arctic exhibits more moderate increases, with the smallest change observed in Iceland (+79%).

An elevation-based analysis of changes in the fraction of extreme runoff within Greenland between the 1980–2000 and 2000–2020 periods reveal a consistent upward trend across all elevations and subregions (figure 4). The mean fraction of extreme runoff increased from 8% in 1980–2000 to 30% in 2000–2020 across all Greenland sectors. An increase of the fraction of extreme runoff towards higher elevation areas suggests that new areas previously less affected have become increasingly prone to extreme melt events in recent decades. However, the magnitude of these changes varies across subregions. The North-West (NW) area experienced the most pronounced increase, particularly at higher elevations. At

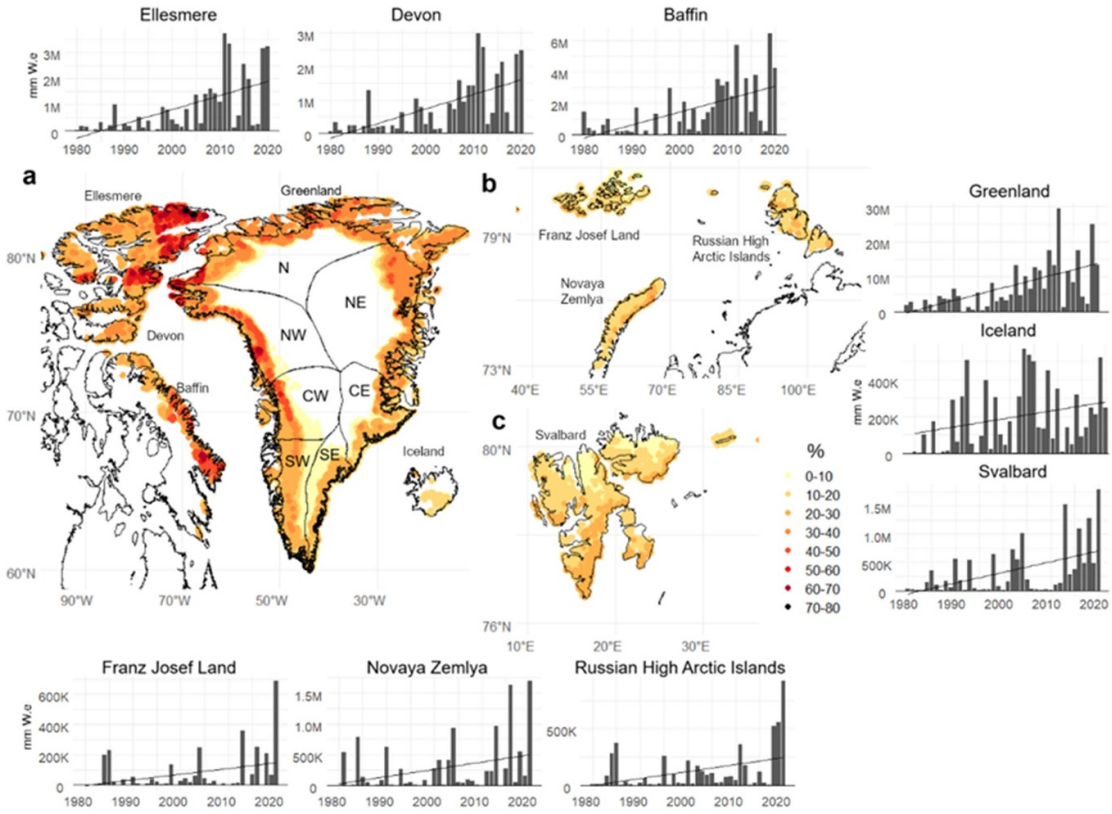

Figure 1. The maps display anomalies in the frequency of extreme runoff events, showing the percentage increase in the fraction of extreme runoff from the period 1980–2000 compared to 2000–2020. The spatial domains are grouped as follows: (a) Western Arctic, including Ellesmere, Devon, Baffin, Greenland, and Iceland; (b) Franz Josef Land, Novaya Zemlya, and the Russian High Arctic Islands; and (c) Svalbard. Warmer colors indicate greater increases in the frequency of extreme runoff events. The column plots illustrate the temporal evolution of summer-accumulated runoff (mm w.e.) during extreme runoff months, grouped by region.

1750 m, the fraction of extreme runoff rose by 40.5%, the highest recorded change across all subregions and elevation bands. Similarly, the North (NO) subregion also showed substantial increases, especially in mid-to-high elevations (600–1200 m), where average changes exceeded 30%. The South-West (SW) and Central-West (CW) subregions displayed intermediate increases, generally ranging from 20% to 30%. In contrast, the Central-East (CE) and especially the South-East (SE) subregions exhibited the smallest increases. Some elevations in these areas showed relatively modest increases in the fraction of extreme runoff, with shifts of around 15%.

To assess regional trends in mid-tropospheric circulation that could explain these changes, Z500 summer evolution is analyzed over the Arctic. Results indicate a pronounced increase in Z500 across the West Arctic (figures 5(a) and (b)). Particularly, statistically significant upward trends ($p < 0.05$) are found across much of the West Arctic domain. In contrast, no statistically significant trends are observed over the East Arctic. Anomalies with respect to the 1980–2000 period confirm a higher increase in the West Arctic than in the East (figure 5(c)), with peaks in years such as 2012 and 2019 coinciding with extreme melt summers in GrIS (Bonsoms *et al* 2024).

4. Discussion

The fraction of extreme runoff, total quantity and spatial extent have all increased across the Arctic. However, distinct regional trends are evident. These variations can be attributed to differences in topography, the extent of melt-prone areas, and the influence of atmospheric circulation patterns and trends.

4.1. Spatial variability of extreme runoff trends in permanent land ice areas

Arctic amplification is a fundamental driver behind the observed increase in extreme runoff events, with rising temperatures and feedback mechanisms accelerating melt processes across the region (Cohen *et al* 2014, Chung *et al* 2021, You *et al* 2021). One of the most key findings of this analysis is the clear regional differentiation in extreme runoff trends. The Western Arctic—including Greenland, Baffin, and Ellesmere—shows the most pronounced increases in both the fraction of extreme runoff and total runoff volume. The Mann–Kendall test confirms statistically significant trends at the 95th and 99th percentiles, indicating a long-term shift toward higher runoff volumes and more persistent extreme events. This amplification is particularly evident in

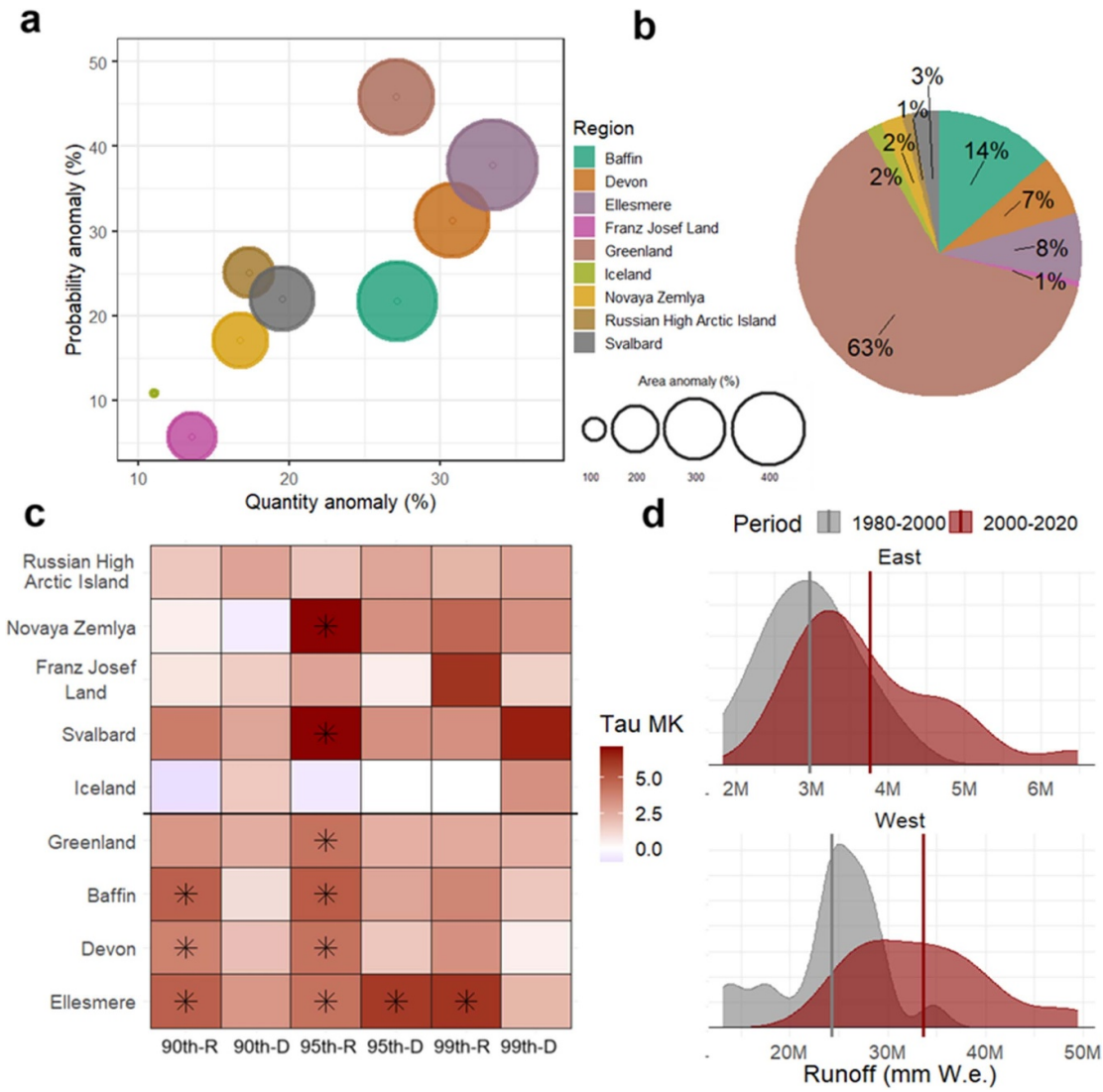

Figure 2. Multidimensional assessment of extreme runoff trends across Arctic regions. (a) Relationship between anomalies in the fraction of extreme runoff (y-axis), quantity of extreme runoff (x-axis), and spatial extent (indicated by point size). Anomalies are expressed as percentage changes between the 1980–1999 and 2000–2020 periods.(b) Regional distribution of the percentage of extreme runoff occurrence across Arctic regions during the 2000–2020 period. (c) Sensitivity analysis of the fraction of extreme runoff based on different percentile thresholds (90th, 95th, 99th), comparing non-detrended (−R) and detrended (−D) data. Statistically significant trends ($p < 0.05$) are indicated by stars. (d) Probability density functions (PDFs) of accumulated runoff for the 1980–2000 (gray) and 2000–2020 (red) periods, shown separately for Eastern and Western Arctic regions.

Western Arctic regions, where Greenland, Ellesmere, and Devon exhibit the largest increases in the fraction of extreme runoff (+46%, +38%, and +31%, respectively), accompanied by substantial expansions in the affected area (figures 2 and 3). The consistent trends across methods and detrended/non-detrended datasets indicate that alternative temporal groupings, rather than the 20 year periods analyzed here, would not substantially alter the conclusions presented. Although SIC is not directly analyzed here but clearly driven by the atmospheric circulation evolution presented in this work (figure 5). These trends align with recent studies showing that Arctic amplification and associated warming rates vary across the region, with faster increases in melting and a negative correlation between summer meltwater and Arctic sea ice in the West Arctic, but no significant relationship in the East Arctic (Maure *et al* 2023) A critical consequence of Arctic amplification is the extension of extreme melt conditions beyond the traditional peak summer season. Observational and model-based studies indicate that the onset and termination of the melt season are shifting, with earlier melt onset and delayed freeze-up contributing to prolonged periods of high air temperature (Giesse *et al* 2024). The results support this trend, as the number of extreme runoff months has increased significantly, particularly in Greenland, Devon, and Ellesmere.

A key factor in understanding future changes in the Arctic SMB is the complex relationship between snowfall and runoff trends. Although snowfall has increased in some regions—such as Franz Josef Land and Novaya Zemlya (+28% from 1995 to 2020) (Maure *et al* 2023)—this increase has not

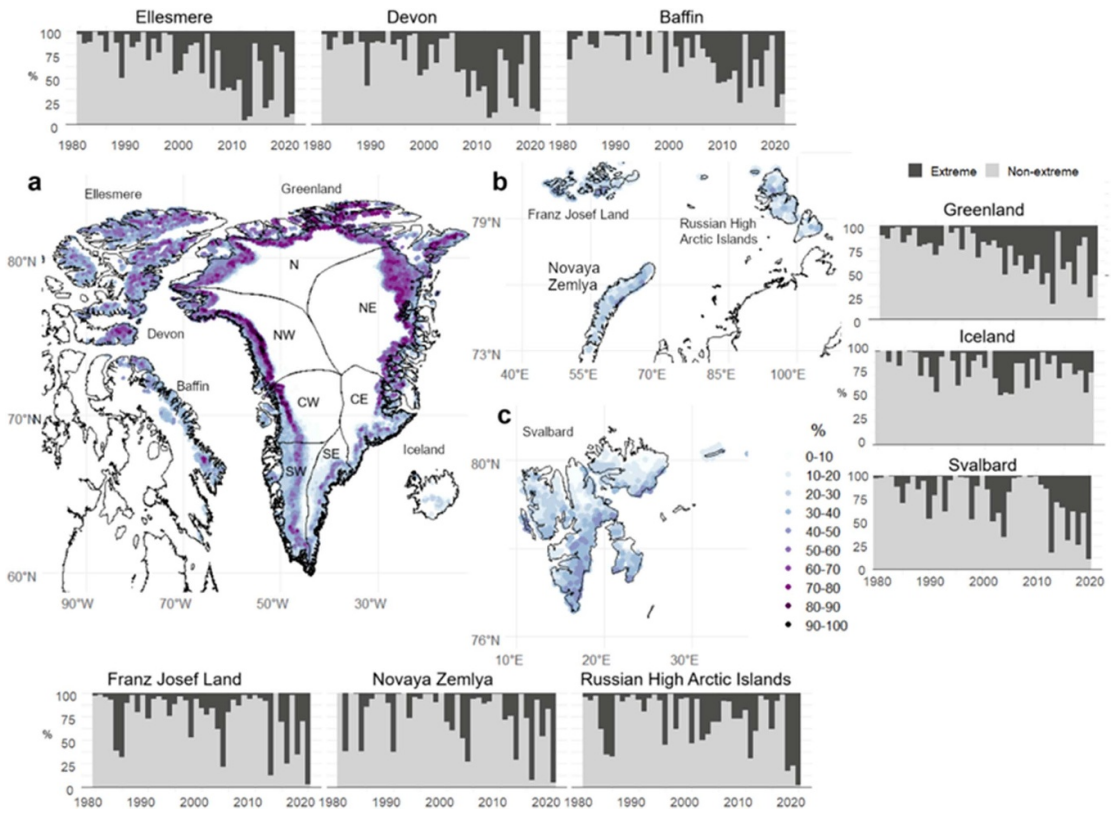

Figure 3. Spatial distribution and temporal evolution of extreme runoff occurrence across the Arctic region. (a) Western Arctic, including Ellesmere, Devon, Baffin, Greenland and Iceland. (b) Russian Arctic sector, including Franz Josef Land, Novaya Zemlya, and the Russian High Arctic Islands and (c) Svalbard. (a) For each panel, the map displays the percentage of extreme runoff occurrence during the 2000–2020 period, with Arctic subregions outlined. Darker colors indicate higher frequencies of extreme runoff. Accompanying bar plots illustrate the temporal evolution of the fraction of extreme runoff events (black bars) and non-extreme events (gray bars) for each region over the full 1980–2020 period.

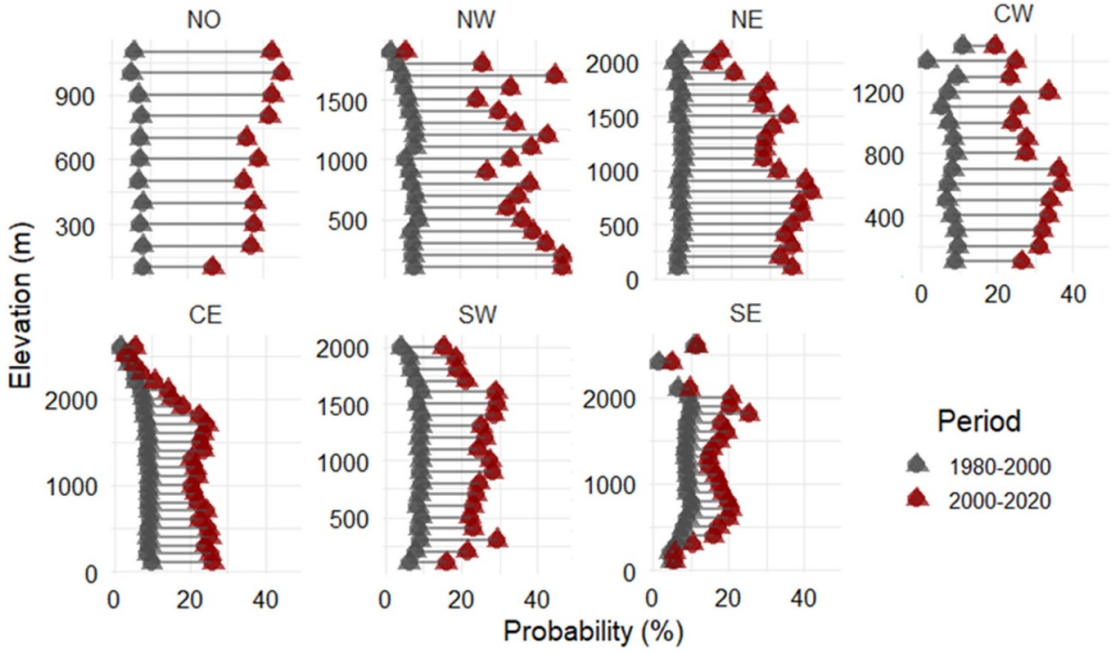

Figure 4. Fraction of extreme runoff in Greenland across elevation bands and time periods. The *x*-axis represents the fraction of extreme runoff (%), while the *y*-axis shows elevation ranges. Colored bars indicate values for two distinct time periods: 1980–2000 and 2000–2020.

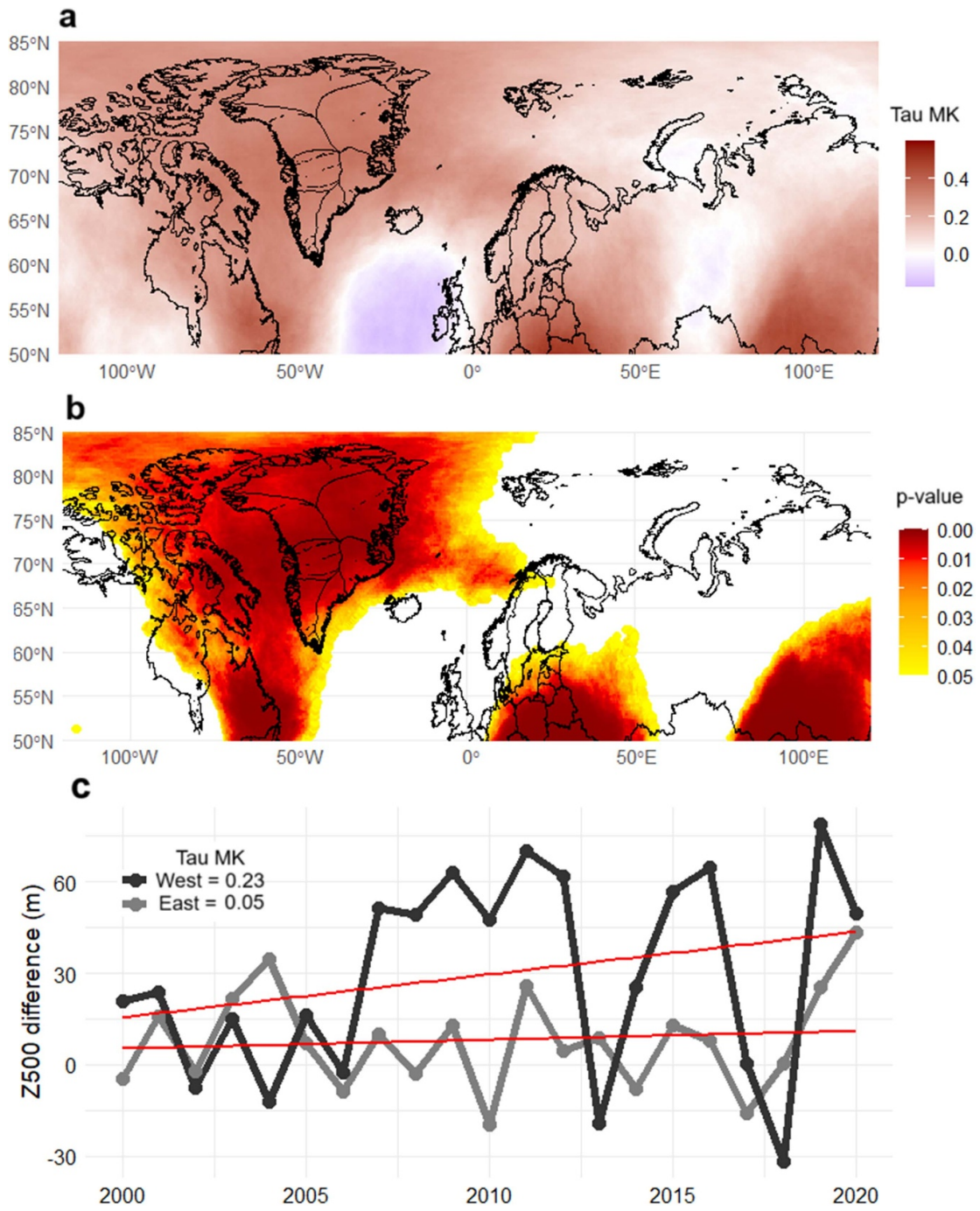

Figure 5. (a) Spatial distribution of the Mann–Kendall Tau trend (Tau MK) in Z500 (m) over the Northern Hemisphere during summer (1980–2020). (b) Corresponding p-values for the trend analysis shown in (a). (c) Time series of Z500 anomalies relative to the 1980–2000 average for the Western and Eastern Arctic regions, with the solid red line representing the linear regression.

been sufficient to counterbalance the acceleration of runoff, leading to negative SMB (Maure *et al* 2023).). Moreover, recent analyses show no significant trend in snowfall across Greenland between 1991 and 2021 (Box *et al* 2023). Shifts in atmospheric circulation patterns, including changes in the Greenland Blocking Index and the North-Atlantic Oscillation (NAO), have increased the persistence of high-pressure systems over Greenland, leading to prolonged warm periods and intensified surface melt (Wachowicz *et al* 2021, Preece *et al* 2023, Hanna *et al* 2014, 2024). Our results go in line with these findings and suggest a westward intensification of high-pressure systems in the Arctic, linked to atmospheric dynamics (figure 5). These circulation anomalies favor the advection of warm southern air along the west coast of Greenland, enhancing melt across the Canadian Arctic and western Greenland. Conversely, northern cold-air advection dominates along Greenland's eastern side, helping explain the observed contrast between Western and Eastern Arctic melting patterns. This west–east

asymmetry is particularly evident in the interannual variability of melt across the GrIS and Svalbard (Lang *et al* 2015). The trend is especially pronounced in NW Greenland, and Ellesmere, where extreme runoff areas have expanded by nearly 400% (figure 4), further increased by the expansion of the ablation zone (Noël *et al* 2019). This combination of enhanced atmospheric circulation patterns and ablation zone expansion has increased radiation absorption and sublimation rates, further accelerating melt, particularly in northern GrIS (Bonsoms *et al* 2024). In contrast, the Eastern Arctic shows more variable and less pronounced trends. Some regions, such as Franz Josef Land (+2%) and Iceland (+11%), show modest increases in the fraction of extreme runoff, while others, including Svalbard and Novaya Zemlya, display statistically significant trends only at higher percentiles Larger extreme runoff changes in NW, CW and SW Greenland are driving accelerated runoff trends, whereas SE and CE Greenland show moderate responses. In these eastern regions, steep topography limits melt, and prevailing northern air advection during summer mitigates temperature increases. The SE and CE sectors of Greenland, along with Iceland, are influenced by anticyclonic patterns associated with the NAO dipole, which enhances melting in western Greenland while reducing atmospheric pressure over eastern regions and promoting cooler conditions in the East (Bjørk *et al* 2018). The relative stability of melting in Iceland is partly attributed to the 'Blue Blob'—a cold anomaly in the North Atlantic caused by a weakening of ocean currents that transport warm tropical waters northward—though this pattern is expected to reverse in coming decades (Noël *et al* 2022). Finally, for parts of the Russian Arctic, such as Franz Josef Land, where specific atmospheric circulation trends are less well-documented, changes in extreme runoff are likely influenced by localized oceanic feedback that buffer warming (Maure *et al* 2023).

Since the largest and most statistically significant increases were found in the raw (non-detrended) runoff data, our results suggest that extreme runoff has intensified alongside long-term increases in runoff. Future research should aim to compare runoff trends directly with global warming levels. While previous studies have shown that temperature extremes tend to increase approximately linearly with global mean warming (IPCC 2022), the frequency of extreme temperature events in the Arctic has been found to follow an exponential trend (Giesse *et al* 2024). A similar analysis focused on future runoff extremes would be valuable to determine whether they exhibit comparable nonlinear behavior in response to warming.

4.2. Implications of rising extreme runoff trends

The long-term implications of these changes remain uncertain, but they highlight the need for continued monitoring and the development of improved physically based models to better assess the evolving Arctic hydrological cycle. In addition to altering ocean stratification and circulation, increased extreme runoff can accelerate terrestrial erosion and sediment transport, reshaping Arctic drainage basins and delivering nutrients and fine particulates to the Arctic Ocean (Zhang *et al* 2022, Chartrand *et al* 2023). These processes may also enhance localized permafrost thaw and carbon release from periglacial sediments, introducing additional positive feedbacks to Arctic warming and increasing the vulnerability of Arctic infrastructure that crosses rivers and floodplains (Moon *et al* 2019). The rising fraction of extreme runoff events could also lead to more frequent flooding and coastal erosion (Landrum and Holland 2020), particularly in Greenland and northern Canada, where communities are increasingly vulnerable due to their reliance on stable ice conditions for transportation and resource extraction (Ford *et al* 2021). Reduced sea ice cover and increased runoff are fundamentally altering ocean–atmosphere heat exchange processes in the Arctic (Huang *et al* 2021). Modeled increases in extreme runoff are also contributing to changes in surface ocean stratification, intensifying ocean warming and the occurrence of marine heatwaves (Gou *et al* 2025). The intensification of extreme runoff has profound implications for Arctic hydrology, ecosystems, and global climate systems. Increased freshwater input into the Arctic Ocean is altering salinity gradients, with cascading effects on nutrient cycling, primary productivity, and the broader Arctic food web (Nummelin *et al* 2016). These changes affect the distribution and abundance of key marine species and can shift oceanographic circulation patterns. Moreover, as extreme runoff events become more frequent and persistent, they contribute significantly to the freshwater flux into the Arctic Ocean and to global sea-level rise (Box *et al* 2018). The acceleration of extreme runoff from Greenland and the Canadian Arctic Archipelago also poses a potential threat to the AMOC, a critical component of global climate regulation, and North Atlantic storm track behavior (Swingedouw *et al* 2022, Van Westen *et al* 2024).

5. Conclusions

Extreme runoff events in the permanent land ice areas of the Arctic have intensified over the past four decades, with clear increases in frequency, magnitude, and spatial extent. The Western Arctic shows the strongest increases across all extreme runoff indicators, with an expansion into new melt-prone areas, influenced largely by changes in atmospheric circulation that favor southern warm air advection into the region during summer. Regional differences are particularly pronounced, highlighting the complex interplay between climate dynamics, topography, and

hydrological responses across the Arctic. The main findings of this study are summarized as follows:

1. Substantial increases in extreme runoff: Greenland (+46%), Ellesmere (+38%), and Devon (+31%) exhibit the strongest increases in the fraction of extreme runoff when comparing 1980–2000–2000–2020, with the spatial extent of affected areas expanding by up to 400% in Ellesmere.
2. Marked West–East contrast: The greatest increases in extreme runoff quantity occurred in Ellesmere (+33%), Devon (+32%), and Greenland (+27%) between 1980–2000 and 2000–2020, consistent with stronger warming and more persistent high-pressure anomalies in the Western Arctic. In contrast, the Eastern Arctic showed more moderate changes, with Iceland (+11%) and Franz Josef Land (+2%) showing the smallest increases.
3. Expansion into new melt-prone areas: Greenland accounts for 63% of the total extreme runoff across Arctic regions. The mean fraction of extreme runoff across Greenland's subregions increased from 8% (1980–2000) to 30% (2000–2020), with values exceeding 40% (2000–2020) modeled in specific elevation bands of NW Greenland.

These findings enhance our understanding of extreme climate trends in the Arctic and underscore their far-reaching impacts on regional hydrology, ecosystems, oceanographic dynamics, and global climate feedback mechanisms.

Data availability statement

All data that support the findings of this study are included within the article (and any supplementary files).

Acknowledgment

This work falls within the NEOGREEN (PID2020-113798GB-C31), ISLANDSINTHEICE (CNS2023-144040) and GRELARCTIC (PID2023-146730NB-C31) projects coordinated by the ANTALP research group (2021 SGR 00269). J B is supported by a pre-doctoral FPI Grant (PRE2021097046) funded by the Spanish Ministry of Science, Innovation and Universities. Marc Oliva acknowledges support from the ICREA Academia program.

Author contributions

Josep Bonsoms 0000-0001-8180-9095
Conceptualization (lead), Data curation (lead), Formal analysis (lead), Funding acquisition (supporting), Investigation (lead), Methodology (lead), Project administration (supporting), Resources (lead), Software (lead), Supervision (lead), Validation (lead), Visualization (lead), Writing – original draft (lead), Writing – review & editing (lead)

Xavier Fettweis 0000-0002-4140-3813
Investigation (supporting), Methodology (supporting), Software (supporting), Writing – review & editing (supporting)

Marc Oliva 0000-0001-6521-6388
Funding acquisition (lead), Project administration (lead), Writing – review & editing (supporting)

Sergi González-Herrero 0000-0002-2505-2435
Methodology (supporting), Writing – review & editing (supporting)

Ignacio López-Moreno 0000-0002-7270-9313
Project administration (supporting), Supervision (supporting), Writing – review & editing (supporting)

References

Bjørk A A *et al* 2018 Changes in Greenland's peripheral glaciers linked to the North Atlantic Oscillation *Nat. Clim. Change* **8** 48–52

Boers N 2021 Observation-based early-warning signals for a collapse of the Atlantic meridional overturning circulation *Nat. Clim. Change* **11** 680–8

Bonsoms J, Oliva M, López-Moreno J I and Fettweis X 2024 Rising extreme meltwater trends in Greenland ice sheet (1950–2022): surface energy balance and large-scale circulation changes *J. Clim.* **37** 4851–66

Boon S, Sharp M and Nienow P 2003 Impact of an extreme melt event on the runoff and hydrology of a high Arctic glacier *Hydrol. Process.* **17** 1051–72

Box J E *et al* 2023 Greenland ice sheet rainfall climatology, extremes and atmospheric river rapids *Meteorol. Appl.* **30** e2134

Box J E, Colgan W T, Wouters B, Burgess D O, O'Neel S, Thomson L I and Mernild S H 2018 Global sea-level contribution from Arctic land ice: 1971–2017 *Environ. Res. Lett.* **13** 125012

Brun E, David P, Sudul M and Brunot G 1992 A numerical model to simulate snow-cover stratigraphy for operational avalanche forecasting *J. Glaciol.* **38** 13–22

Callaghan T V *et al* 2011 The changing face of arctic snow cover: a synthesis of observed and projected changes *Ambio* **40** 17–31

Chartrand S M, Jellinek A M, Kukko A, Galofre A G, Osinski G R and Hibbard S 2023 High Arctic channel incision modulated by climate change and the emergence of polygonal ground *Nat. Commun.* **14** 5297

Chung E S, Ha K J, Timmermann A, Stuecker M F, Bodai T and Lee S K 2021 Cold-season Arctic amplification driven by Arctic Ocean-mediated seasonal energy transfer *Earths Future* **9**

Cohen J *et al* 2014 Recent Arctic amplification and extreme mid-latitude weather *Nat. Geosci.* **7** 627–37

Coumou D, Di Capua G, Vavrus S, Wang L and Wang S 2018 The influence of Arctic amplification on mid-latitude summer circulation *Nat. Commun.* **9** 2959

Delhasse A, Kittel C, Amory C, Hofer S, Van As D, Fausto R S and Fettweis X 2020 Brief communication: evaluation of the near-surface climate in ERA5 over the Greenland Ice Sheet *Cryosphere* **14** 957–65

Dobricic S, Russo S, Pozzoli L, Wilson J and Vignati E 2020 Increasing occurrence of heat waves in the terrestrial Arctic *Environ. Res. Lett.* **15** 024022
Fettweis X *et al* 2020 GrSMBMIP: intercomparison of the modelled 1980–2012 surface mass balance over the Greenland ice sheet *Cryosphere* **14** 3935–58
Fichot C G, Kaiser K, Hooker S B, Amon R M W, Babin M, Bélanger S, Walker S A and Benner R 2013 Pan-Arctic distributions of continental runoff in the Arctic Ocean *Sci. Rep.* **3** 1053
Ford J D, Pearce T, Canosa I V and Harper S 2021 The rapidly changing Arctic and its soci*et al* implications *Wiley Interdiscip. Rev. Clim. Change* **12** e735
Francis J and Skific N 2015 Evidence linking rapid Arctic warming to mid-latitude weather patterns *Phil. Trans. R. Soc. A* **373** 20140170
Gallée H and Schayes G 1994 Development of a three-dimensional meso-γ primitive equation model: katabatic winds simulation in the area of Terra Nova Bay, Antarctica *Mon. Wea. Rev.* **122** 671–85
Giesse C, Notz D and Baehr J 2024 The shifting distribution of Arctic daily temperatures under global warming *Earths Future* **12** e2024EF004961
Gou R, Wolf K K E, Hoppe C J M, Wu L and Lohmann G 2025 The changing nature of future Arctic marine heatwaves and its potential impacts on the ecosystem *Nat. Clim. Change* **15** 162–70
Hanna E *et al* 2024 Short- and long-term variability of the Antarctic and Greenland ice sheets *Nat. Rev. Earth Environ.* **5** 193–210
Hanna E, Fettweis X, Mernild S H, Cappelen J, Ribergaard M H, Shuman C A, Steffen K, Wood L and Mote T L 2014 Atmospheric and oceanic climate forcing of the exceptional Greenland ice sheet surface melt in summer 2012 *Int. J. Climatol.* **34** 1022–37
Hanna E, Hall R J and Overland J E 2017 Can Arctic warming influence UK extreme weather? *Weather* **72** 346–52
Hansen B B, Isaksen K, Benestad R E, Kohler J, Pedersen Å, Loe L E, Coulson S J, Larsen J O and Varpe Ø 2014 Warmer and wetter winters: characteristics and implications of an extreme weather event in the high Arctic *Environ. Res. Lett.* **9** 114021
Hersbach H *et al* 2020 The ERA5 global reanalysis *Q. J. R. Meteorol. Soc.* **146** 1999–2049
Hjort J, Karjalainen O, Aalto J, Westermann S, Romanovsky V E, Nelson F E, Etzelmüller B and Luoto M 2018 Degrading permafrost puts Arctic infrastructure at risk by mid-century *Nat. Commun.* **9** 5147
Huang B, Wang Z, Yin X, Arguez A, Graham G, Liu C, Smith T and Zhang H M 2021 Prolonged marine heatwaves in the Arctic: 1982−2020 *Geophys. Res. Lett.* **48** e2021GL095590
Hugonnet R *et al* 2021 Accelerated global glacier mass loss in the early twenty-first century *Nature* **592** 726–31
IPCC 2022 High mountain areas *The Ocean and Cryosphere in a Changing Climate* (Cambridge University Press) pp 131–202
Kendall M G 1975 *Rank Correlation Methods* 4th edn (Charles Griffin)
Landrum L and Holland M 2020 Extremes become routine in an emerging new Arctic *Nat. Clim. Change* **10** 1108–15
Lang C, Fettweis X and Erpicum M 2015 Stable climate and surface mass balance in Svalbard over 1979–2013 despite the Arctic warming *Cryosphere* **9** 83–101
Lenton T M, Held H, Kriegler E, Hall J W, Lucht W, Rahmstorf S and Schellnhuber H J 2008 Tipping elements in the Earth's climate system *Proc. Natl Acad. Sci.* **105** 1786–93
Liston G E and Hiemstra C A 2011 The changing cryosphere: pan-Arctic snow trends (1979–2009) *J. Clim.* **24** 5691–712
Machguth H, Macferrin M, Van As D, Box J E, Charalampidis C, Colgan W, Fausto R S, Meijer H A J, Mosley-Thompson E and Van De Wal R S W 2016 Greenland meltwater storage in firn limited by near-surface ice formation *Nat. Clim. Change* **6** 390–3
Mann H B 1945 Nonparametric tests against trend *Econometrica* **13** 245–59
Matthes H, Rinke A and Dethloff K 2016 Corrigendum: recent changes in Arctic temperature extremes: warm and cold spells during winter and summer (2015 Environ. Res. Lett. 10 114020) *Environ. Res. Lett.* **11** 2015 *Environ. Res. Lett. 10 114020* **11** 029501
Maure D, Kittel C, Lambin C, Delhasse A and Fettweis X 2023 Spatially heterogeneous effect of climate warming on the Arctic land ice *Cryosphere* **17** 4645–59
Miner K R, Turetsky M R, Malina E, Bartsch A, Tamminen J, McGuire A D, Fix A, Sweeney C, Elder C D and Miller C E 2022 Permafrost carbon emissions in a changing Arctic *Nat. Rev. Earth Environ.* **3** 55–67
Moon T A *et al* 2019 The expanding footprint of rapid Arctic change *Earth's Future* **7** 212–8
Noël B, Aðalgeirsdóttir G, Pálsson F, Wouters B, Lhermitte S, Haacker J M and van den Broeke M R 2022 North Atlantic cooling is slowing down mass loss of icelandic glaciers *Geophys. Res. Lett.* **49** e2021GL095697
Noël B, Van De Berg W J, Lhermitte S and Van Den Broeke M R 2019 Rapid ablation zone expansion amplifies north Greenland mass loss *Adv. Sci.* **5** eaaw0123
Nummelin A, Ilicak M, Li C and Smedsrud L H 2016 Consequences of future increased Arctic runoff on Arctic Ocean stratification, circulation, and sea ice cover *J. Geophys. Res.* **121** 617–37
Preece J R, Mote T L, Cohen J, Wachowicz L J, Knox J A, Tedesco M and Kooperman G J 2023 Summer atmospheric circulation over Greenland in response to Arctic amplification and diminished spring snow cover *Nat. Commun.* **14** 3759
Pulliainen J *et al* 2020 Patterns and trends of Northern Hemisphere snow mass from 1980 to 2018 *Nature* **581** 294–8
Rantanen M, Karpechko A Y, Lipponen A, Nordling K, Hyvärinen O, Ruosteenoja K, Vihma T and Laaksonen A 2022 The Arctic has warmed nearly four times faster than the globe since 1979 *Commun. Earth Environ.* **3** 168
Rignot E and Mouginot J 2012 Ice flow in Greenland for the international polar year 2008–2009 *Geophys. Res. Lett.* **39** 11
Sasgen I, Steinhoefel G, Kasprzyk C, Matthes H, Westermann S, Boike J and Grosse G 2024 Atmosphere circulation patterns synchronize pan-Arctic glacier melt and permafrost thaw *Commun. Earth Environ.* **5** 375
Sen P K 1968 Estimates of the regression coefficient based on Kendall's tau *J. Am. Stat. Assoc.* **63** 1379–89
Sharp M, Burgess D O, Cogley J G, Ecclestone M, Labine C and Wolken G J 2011 Extreme melt on Canada's Arctic ice caps in the 21st century *Geophys. Res. Lett.* **38** L11501
Swingedouw D, Houssais M N, Herbaut C, Blaizot A C, Devilliers M and Deshayes J 2022 AMOC recent and future trends: a crucial role for oceanic resolution and Greenland melting? *Front. Clim.* **4** 838310
Tang Q, Zhang X and Francis J A 2014 Extreme summer weather in northern mid-latitudes linked to a vanishing cryosphere *Nat. Clim. Change* **4** 45–50
Tedesco M and Fettweis X 2020 Unprecedented atmospheric conditions (1948–2019) drive the 2019 exceptional melting season over the Greenland ice sheet *Cryosphere* **14** 1209–23
van der Wiel K and Bintanja R 2021 Contribution of climatic changes in mean and variability to monthly temperature and precipitation extremes *Commun. Earth Environ.* **2** 1
Van Westen R M, Kliphuis M and Dijkstra H A 2024 Physics-based early warning signal shows that AMOC is on tipping course *Sci. Adv.* **10** eadk1189
Wachowicz L J, Preece J R, Mote T L, Barrett B S and Henderson G R 2021 Historical trends of seasonal Greenland blocking under different blocking metrics *Int. J. Climatol.* **41** E3263–78
Walsh J E, Ballinger T J, Euskirchen E S, Hanna E, Mård J, Overland J E, Tangen H and Vihma T 2020 Extreme weather

and climate events in northern areas: a review *Earth Sci. Rev.* **209** 103324

Walsh J E, Bieniek P A, Brettschneider B, Euskirchen E S, Lader R and Thoman R L 2017 The exceptionally warm winter of 2015/16 in Alaska *J. Clim.* **30** 2069–88

You Q *et al* 2021 Warming amplification over the Arctic pole and third pole: trends, mechanisms and consequences *Earth Sci. Rev.* **217** 103625

Yue S, Pilon P and Phinney B O B 2003 Canadian streamflow trend detection: impacts of serial and cross-correlation *Hydrol. Sci. J.* **48** 51–63

Zhang T, Li D, East A E, Walling D E, Lane S, Overeem I, Beylich A A, Koppes M and Lu X 2022 Warming-driven erosion and sediment transport in cold regions *Nat. Rev. Earth Environ.* **3** 261–79